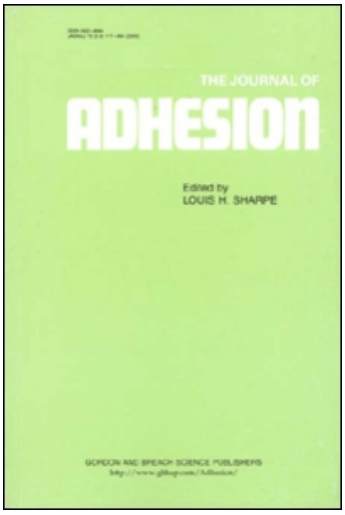

The Journal of Adhesion
Publication details, including instructions for authors and subscription information:
http://www.informaworld.com/smpp/title~content=t713453635

The Adhesion of Carbon Fibers to Thermoset and Thermoplastic Polymers

W. D. Bascom[a]; K-J. Yon[ab]; R. M. Jensen[c]; L. Cordner[c]
[a] Department of Materials Science and Engineering, 304 EMRO, University of Utah, Salt Lake City, UT, U.S.A. [b] University of Wisconsin, Madison, WI [c] Hercules Aerospace, Magna, UT, U.S.A.

To cite this Article Bascom, W. D. , Yon, K-J. , Jensen, R. M. and Cordner, L.(1991) 'The Adhesion of Carbon Fibers to Thermoset and Thermoplastic Polymers', The Journal of Adhesion, 34: 1, 79 — 98
To link to this Article: DOI: 10.1080/00218469108026507
URL: http://dx.doi.org/10.1080/00218469108026507

J. Adhesion, 1991, Vol. 34, pp. 79–98
Reprints available directly from the publisher
Photocopying permitted by license only

Printed in the United Kingdom

The Adhesion of Carbon Fibers to Thermoset and Thermoplastic Polymers

W. D. BASCOM† and K-J. YON‡

Department of Materials Science and Engineering, 304 EMRO, University of Utah, Salt Lake City, UT 84112, U.S.A.

R. M. JENSEN, and L. CORDNER

Hercules Aerospace, Magna, UT 84044, U.S.A.

(Received March 6, 1990, in final form December 29, 1990)

The adhesion of three carbon fibers, AS1, AS4, and XAS to thermosetting and thermoplastic polymers has been investigated using the single, embedded filament test. All three fiber types exhibited strong adhesion to the thermosets (epoxies) whereas only the XAS bonded strongly to the thermoplastics. Common explanations for low adhesion, such as weak boundary layers and surface roughness, were investigated and shown not to be responsible for the differences in adhesion. Different levels of fiber surface treatment and various organic sizings also had no effect. Surface analysis of the fibers using XPS and retention time chromatography indicate a subtle difference in the surface chemical constitution of the three fibers but the exact nature of these differences was not determined.

KEY WORDS Carbon fiber composites; thermoplastic matrix composites; fiber/matrix adhesion; single embedded fiber adhesion test; retention time chromatography; stress birefringence.

INTRODUCTION

In general, thermosetting polymers adhere more strongly to carbon fibers than do thermoplastic polymers. Evidence for these differences in adhesion is based primarily on scanning electron microscopy (SEM) of failed carbon fiber reinforced polymer (CFRP) composites. The fibers in SEM photomicrographs of epoxy and other thermosetting polymer composites are coated with the matrix polymer whereas in similar SEM photographs of thermoplastic matrix composites the fibers appear to have been cleanly separated from the matrix.[1,2] It is possible, of course, that in the case of the thermoplastic matrix composites there is a thin uniform film of polymer on the fibers. However, the difference in the SEM appearance of the thermoset matrix materials compared with the thermoplastic-

† To whom correspondence should be addressed.
‡ Present Address, University of Wisconsin, Madison WI.

based composites is strongly suggestive of a marked difference in fiber-matrix adhesion.

There is some evidence for differences in the mechanical properties of thermoset *vs* thermoplastic matrix composites. Hunston *et al.*[3] compared the interlaminar fracture energy as a function of the matrix fracture energy (G_{1c}) and found that thermoplastic CFRPs did not fit the general trend exhibited by thermoset matrix composites.

This difference in adhesion is not necessarily universal. Scanning electron microscopy of composites with highly cross-linked epoxy and bismaleimide matrices suggest interfacial failure.[4] These observations may be due to limitations in the resolution of the SEM or to micromechanical effects that focus failure into the interfacial region but not actually at the interface. Early development efforts to produce laminates using off-the-shelf polyetheretherketone (PEEK) film and standard carbon fiber resulted in laminates with poor fiber/matrix bonding.[5] Since then, commercial composites of carbon fiber and PEEK (APC2, ICI Ltd, Wilton, UK) exhibit good fiber-matrix adhesion but proprietary processing methods are used to achieve strong bonding.

In the work reported here, the adhesion of three carbon fibers to epoxy polymers and to a variety of thermoplastic polymers are compared using the single embedded filament test.[6-11] All three fibers exhibited strong adhesion to the epoxies but only one exhibited strong adhesion to the thermoplastics. The thrust of this work was to determine the reason(s) for the differences in adhesion to the thermoplastics.

EXPERIMENTAL

Materials

The carbon fibers were AS1 and AS4 supplied by Hercules Aerospace (Magna UT, U.S.A.) and an experimental fiber XAS (Hysol Grafil, Anaheim, CA, U.S.A.) obtained from the NASA Langley Research Center (Hampton, VA, U.S.A). The properties of the fibers are given in Table I taken from company literature. Although the strength of AS4 and XAS are quoted to be essentially equivalent, in handling of the XAS it was qualitatively more fragile than the AS4. Single spools for each fiber were used throughout this investigation unless otherwise indicated.

In Tables II and III the composition and mechanical properties of the polymers studied are listed and, in the case of the thermoplastics (Table III), the solvents and drying conditions used to prepare test specimens (see Procedures). The polymers were used as received from the manufacturer.

Specimen preparation and testing

The embedded single filament test involves encapsulating a fiber in a miniature "dogbone" of polymer. This specimen is then pulled in tension on a micro-tensile

TABLE I
Carbon fiber properties

Fiber designation	Diameter d, μm	0° Laminate tensile properties Strength MPa (ksi)	Modulus GPa (Msi)	Elongation
AS1[a]	8.0	3103 (450)	228 (33)	1.32
AS4[a]	6.84	3587 (520)	235 (34)	1.53
XAS[b]	6.64	3447 (500)	230 (33)	1.67

[a] Hercules Aerospace.
[b] Hysol Grafil.

TABLE II
Epoxy polymers

Designation	Epoxide	Curing agent	Tensile properties Strength MPa (ksi)	Modulus MPa (ksi)
DGEBA/m-PDA	Shell 828	m-phenylene diamine	127 (18.5)*	3620 (523)
DGEBA/ polyanine	Shell 828	polyoxypropyl amine (Jeffamine D230)	64 (9.3)	2614 (379)

DGEBA = diglycidylether of Bisphenol A; m-PDA = meta-phenylene diamine.
* H. Lee and K. Neville, *Handbook of Epoxy Resins* (McGraw Hill, Inc., New York, 1967), p. 14–20.

TABLE III
Thermoplastic polymers

Polymer	Drying conditions Solvent	Time/Temperature	Tensile properties Strength MPa (ksi)	Modulus MPa (ksi)
polycarbonate[a]	methylene chloride	24 hr @ 25°C 16 hr @ 75°C	65 (95)	2400 (345)
polyphenylene oxide (PPO)	methylene chloride /dichloroethane 1/1 ratio	4 hr @ 25°C 16 hr @ 81°C	48 (70)	2200 (325)
polyetherimide[b]	methylene chloride	4 hr @ 25°C 16 hr @ 75°C	105 (152)	2963 (430)
polysulfone[c]	methylene chloride	24 hr @ 25°C 16 hr @ 75°C	70 (101)	2540 (365)
PPO/polystyrene 25/75 wt. ratio	methylene chloride /dichloroethene 1/1 ratio	4 hr @ 25°C 24 hr @ 81°C	ND	ND

[a] Lexan 101, General Electric Co.
[b] ULTEM, General Electric Co.
[c] UDEL, Union Carbide Corp.

machine on the stage of a light optics microscope. With increasing tension the fiber fragments until the fragment length is equal to or less than the critical length. The average critical length is an inverse measure of the fiber matrix adhesion strength. The technique was first used by Kelly and Tyson[6] and later used by Fraser *et al.*[7,8] to measure the adhesion of glass fibers to polypropylene and by Drzal *et al.* to measure the adhesion of carbon fibers to epoxy polymers.[9,10] Drzal was the first to recognize the value of the stress birefringence patterns at fiber breaks as ancillary information about the fiber matrix adhesion strength. Much of the work reported here utilized methods developed by Drzal and coworkers.

The embedded single filament specimen is shown schematically in Figure 1. The specimen is loaded until the fiber fragmentation is complete. The fragment length is measured and the average length taken to be the critical length. From elementary shear lag analysis[12] the critical length is related to the fiber tensile strength and interfacial shear strength by,

$$\tau_c = \frac{\sigma_c d}{2l_c} \tag{1}$$

where:

τ_c = interphase shear strength
σ_c = fiber strength
d = fiber diameter
l_c = fiber critical length

However, the fiber strength has some statistical distribution, $\Sigma\sigma_c$, so that,

$$\tau_c = \frac{d}{2l_c}\Sigma\sigma_c \tag{2}$$

rearranging,

$$\frac{l_c}{d} = \frac{1}{2\tau_c}\Sigma\sigma_c \tag{3}$$

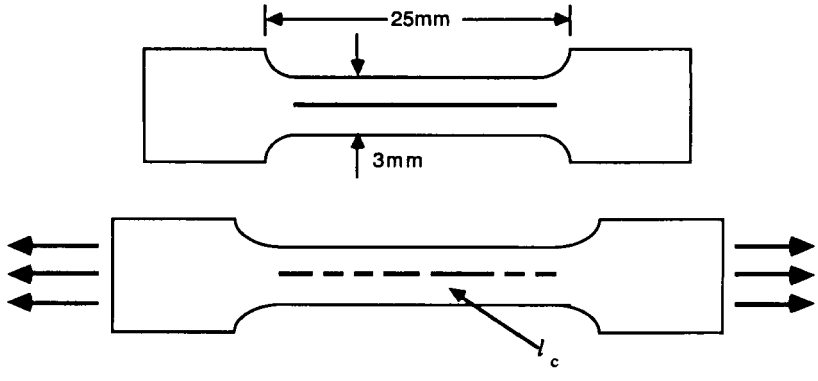

FIGURE 1 Schematic of embedded single filament test specimen.

If the mean and variance of the strength distributions ($\Sigma\sigma_c$) of the fibers being compared are essentially equal then l_c/d, the critical aspect ratio, is an inverse measure of the interphase shear strength. Since all of the fibers compared in this work are "Type II" fibers manufactured under similar conditions, the assumption that they have similar strength distributions is reasonable. Moreover, the differences in critical aspect ratios were large and would be difficult to explain in terms of the fiber strengths alone.

The epoxy test specimens were made by placing the filament in a silicone mold, filling the mold with liquid resin and heat curing. The m-PDA/DGEBA contained 14 phr of amine and was cured at 70°C for 2 hrs and then for three hours at 125°C. The polyanime/DGEBA contained 30 phr of amine† and was cured for two hours at 75°C followed by 125°C for three hours. Further details on specimen preparation are given in Ref. 11.

The thermoplastic specimens were prepared by placing a single filament on a small plate of the polymer and then coating the filament with the same polymer from a volatile solvent (Figure 2). The coating was gently applied using a thin (3 mm) wood applicator until attaining a thickness of at least two fiber diameters. Trials at different coating thicknesses revealed no differences in the critical lengths even when the fiber was less than a fiber diameter below the coating surface. The solvents were removed by drying at the conditions indicated in Table III.

Both the epoxy and thermoplastic specimens were placed in a tensile test fixture that fits on the stage of a light microscope (Figure 3). This test device was designed to have the load applied from both ends of the specimen so that an area of interest remains in the field of view as the specimen is stressed. This feature is a distinct advantage when examining the effect of increasing load on the stress birefringence or other features at a fiber break.

As would be expected from Eq. (3), the critical length exhibits a wide distribution due to the statistical variation of the fiber strength.[11] The data did not

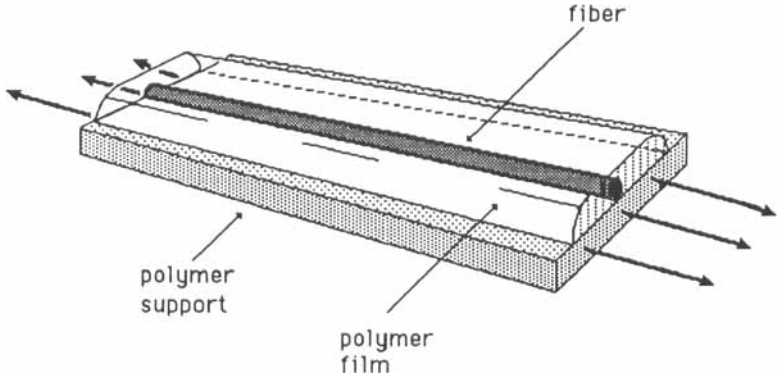

FIGURE 2 Schematic of specimen configuration for testing fibers in thermosplastic polymers.

† A polyoxyalkyleneamine, MW 230 (Jeffamine 230, Texaco).

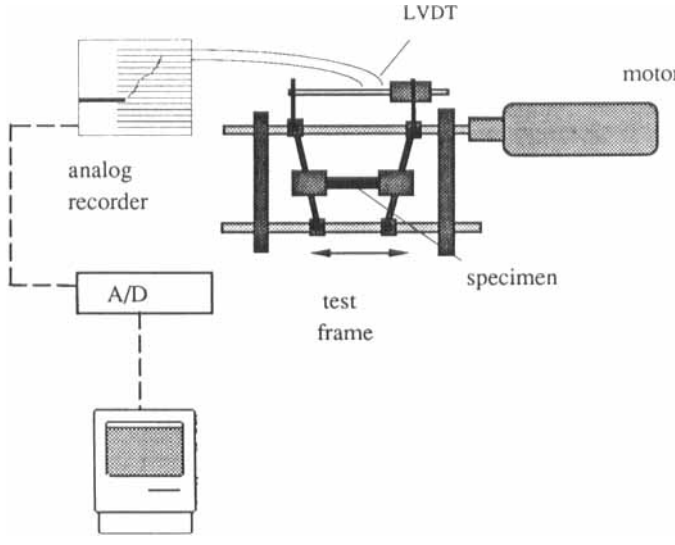

FIGURE 3 Tensile test fixture. The test frame is placed on a microscope stage and can be motor driven and the strain measured using an LVDT displacement transducer.

follow the two-parameter Weibull statistics, so for the data reported here the statistical parameters were determined assuming a normal distribution of fiber fragment lengths. For each fiber/polymer combination 10–12 specimens were tested and the fragment lengths combined and averaged. The statistical variance is reported either as the 99% confidence limits on the mean or as the standard deviation.

All of the polymers in this study were transparent and stress birefringent, so that the experiments revealed information about the stress distribution at fiber breaks. Interpretation of the birefringence patterns was based on classical shear lag theory.[12] There are two conditions of importance; strong bonding between fiber and matrix so that the interfacial shear strength exceeds the matrix shear yield strength and, secondly, low adhesion between fiber and matrix so that the

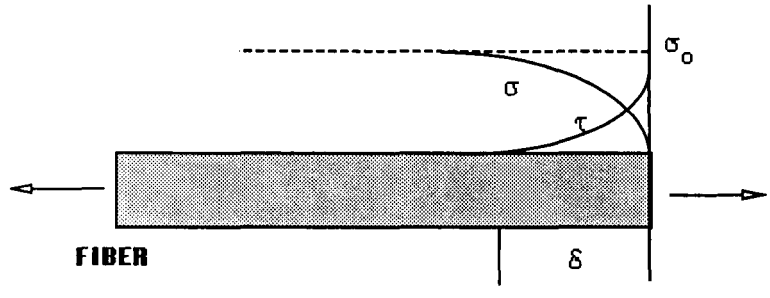

FIGURE 4 Stress distribution at a fiber end under longitudinal loading; σ_0 = far field tensile stress, τ = shear stress and δ = "ineffective" length.

interfacial shear strength is less than the matrix shear yield strength. The elastic stress distribution at a fiber break is illustrated in Fig. 4. The effect of strong adhesion and weak adhesion are illustrated in Fig. 5. The birefringence patterns observed for strong *vs* weak adhesion are shown in Fig. 6 and are distinctly different. The effect of increasing the load on a specimen results in the load redistributions shown in Fig. 5 for strong adhesion (5A) and weak adhesion (5B). In the case of weak adhesion (6B), stress birefringence appears at the fiber breaks but with the slightest increase in load, the birefringent nodes recede from the break as if the matrix was "unzipping" from the fiber. In the case of strong adhesion (6A) the nodes remain close to the fiber break although between the fiber ends and the major node a lip develops with increasing stress. Relaxation of the tension on the specimen causes all of the birefringence to dissipate in the case of weak adhesion whereas the lip of birefringence remains indefinitely in the case of strong adhesion indicating shear yielding.[11]

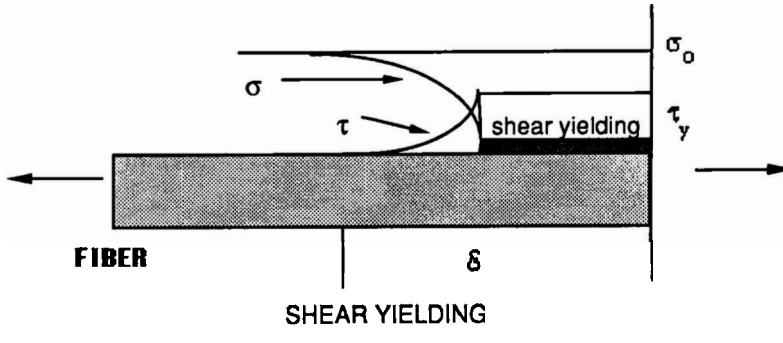

SHEAR YIELDING

A

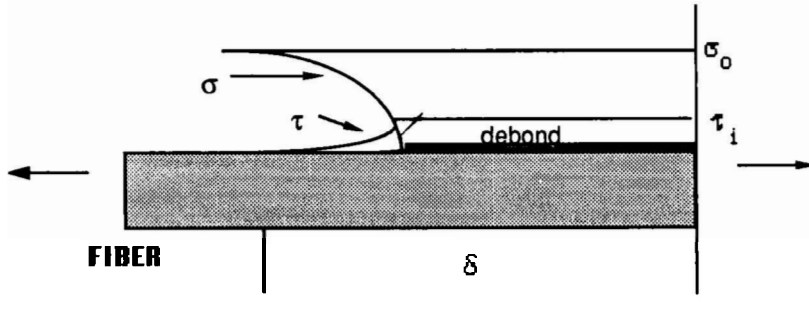

INTERFACIAL FAILURE

FIGURE 5 Schematic of stress distribution for the case of strong adhesion (A) and weak adhesion (B); τ_y and τ_i are the matrix yield strength and the interfacial shear strength respectively.

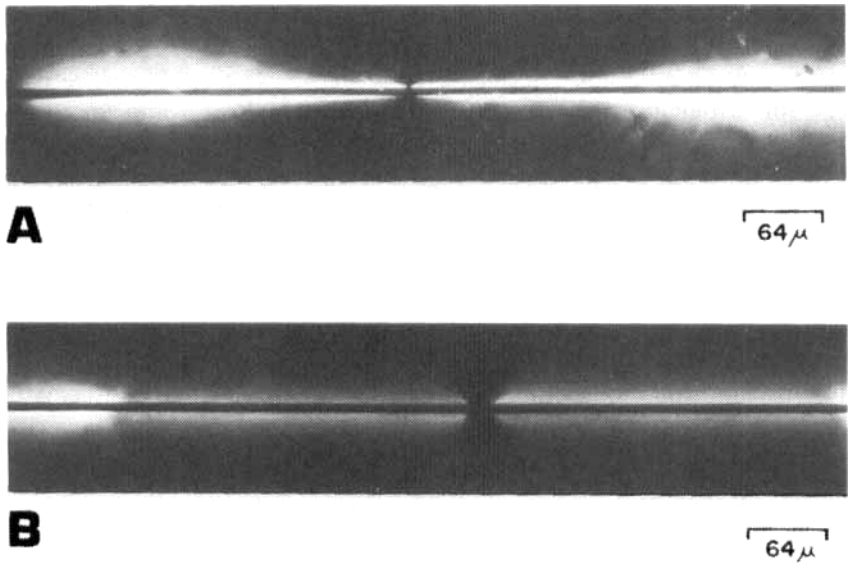

FIGURE 6 Photomicrographs illustrating the stress birefringence at fiber breaks corresponding to strong (A) and weak (B) adhesion.

Surface analyses†

Surface spectroscopy and wettability measurements were used to characterize the carbon fiber surfaces. X-ray photoelectron spectroscopy (XPS) analysis was performed by Surface Science Laboratories (Mountain View, CA, U.S.A.) and at the University of Utah. Contact angle measurements were made using a Wilhelmy tensiometer (Ramé Hart, Mountain Lakes, NJ, U.S.A.).

Fiber surface modification†

Various sizing agents were applied to the carbon fiber as well as variations in surface treatment. The distinction between surface treatment and sizing needs to be emphasized. Commercially-produced carbon fibers are given a surface treatment immediately after the final carbonization/graphitization operations. The surface treatments vary for different manufacturers and are generally a chemical oxidation.

Sizing, on the other hand, is a deliberate coating of the fiber to reduce fiber damage during processing, *e.g.*, prepregging or filament winding. An apparatus was constructed for continuous sizing of a single tow (12 k filaments). The amount of sizing applied to the fiber was controlled by the bath concentration, the speed of the fiber tow, and the temperature in the drying tower. The sizing level was measured by solvent extraction with methylene chloride and weighing of the clean, dried fiber.

† Further details of these procedures can be found in reference 13.

The effect of varying the intensity of the fiber surface treatment on adhesion was studied. The treatment level was set above and below the level used by Hercules Aerospace for commercial carbon fiber products; nominally 100%. Levels of 0% (unsurface treated fiber designated as AU4), 50%, 100% (normal conditions), and 400% were tested. The actual treatment conditions are Hercules proprietary information. The fiber tows were treated in a pilot plant facility using AU4 from production.

Thermal desorption†

Tows of carbon fiber were heat treated to remove thermally desorbable species by passing the tows through a tube furnace at 750°C. The furnace was flushed with nitrogen gas and the fiber residence time was 90s.

Solvent extraction†

Fiber tows were washed with tetrahydrofuran for about 8 hrs using a Soxlet extraction apparatus to remove organic soluble materials from the surface.

Retention time chromatography

A study was made of the retention time of polycarbonate on the three fiber types using high performance liquid chromatography (HPLC). A schematic of the chromatograph is shown in Figure 7. Filament tows of AS4 and XAS carbon fibers, both 12 k, were cut into 150, 2-inch (5 cm) length segments and packed into a chromatography column of 30 cm in length and 1.5 cm internal diameter with a tamping rod. In the case of the AS1 carbon fiber, which was only available in 10 k-filament tows, 180 segments were packed into columns so that each column for the three carbon fibers contained the same amount of filament. The column (Spectrum Medical Industries, Inc.) was constructed of borosilicate glass, and had Teflon® end plates for chemical resistance to organic solvents. The upper end plate had a side vent port in order to expel air from the column.

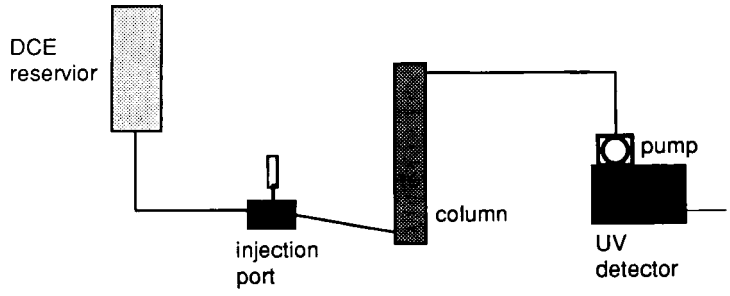

FIGURE 7 Schematic of HPLC chromatograph used for retention time experiments.

Three chromatography columns were prepared for each carbon fiber type to confirm the reproducibility of column packing. After each column was packed it was connected to a flow cell which has a straight-through vertical flow design to expel trapped air bubbles quickly. The column was flushed with the 1,2-dichloroethane solvent to be used for the chromatographic run until all air had been expelled from the column. Since any particulate matter in an unclean solvent can block the fine tubing system inside of the solvent delivery system and sample injector, the solvent was first passed through a membrane filter. The wavelength of the UV detector was set at 265 nm for maximum absorption.

Adsorption of water vapor onto the surface of the carbon fibers could affect the polycarbonate absorption. Therefore, after each column was filled, it was continuously flushed for 12 hours with dry nitrogen gas to remove weakly bound water. The column was then immediately closed with screw caps and placed into a double plastic bag with a desiccant (Drierite), flushed with dry nitrogen gas and sealed until the column was connected to the HPLC system.

With the solvent flowing at a constant rate of 2 ml/min, 0.2 ml of a 1 mg/ml polycarbonate solution was injected using a sample injector that enables one to load and inject samples without interruption of the solvent flow. When an injection is made, a chart recorder automatically marks the injection point on the chromatogram. The retention time was taken at the maximum point of the peak in the UV absorption curve. For each fiber type, five to nine injections were made for each of the three columns which gave 15 to 27 data points.

The chromatographic system used for the retention time measurements was comprised of a model U6K sample injector (Waters Associates), model 590 solvent delivery system (Waters Associates) and a V4 variable wavelength detector (Isco, Inc.) with flow cell. Sentell and Dorsey[14] have discussed retention time in reverse-phase chromatography.

RESULTS

The critical aspect ratios for the three fibers in the epoxy polymers are presented in Table IV. The lower critical aspect ratios for the AS1 and XAS compared with the AS4 can best be explained by differences in the fiber tensile strengths. If we assume in Eq. 3 that the interphase shear strength is essentially constant, then the average critical aspect ratio depends only on the fiber strength. From Table I, the fiber strengths for AS1 and AS4 parallel the critical aspect ratios in the DGEBA/m-PDA epoxy (Table IV). The critical aspect ratio for the XAS is lower than would be expected from the fiber strength quoted by the manufacturer but, as already mentioned, handling of the XAS suggested a lower strength than the AS4.

The critical aspect ratios of the three fibers in the thermoplastic polymers are presented in Tables V-VII. Note that the values for the AS1 and AS4 are significantly higher and the statistical distribution much wider than for the XAS.

TABLE IV
Critical aspect ratio for carbon fiber/epoxy systems

Fiber	Epoxy	Critical aspect ratio, l_c/d Mean	99% confidence limit on mean
AS1[a]	DGEBA/m-PDA	42	—
AS4	DGEBA/m-PDA	55	53–57
AS4	DGEBA/ polyanime	60	58–62
XAS	DGEBA/m-PDA	32	31–33

[a] L. T. Drzal, M. J. Rich, and P. F. Lloyd, *J. Adhesion* **16,** 1 (1983)

TABLE V
Critical aspect ratio for AS4 in thermoplastic polymers

Matrix	Critical aspect ratio, l_c/d Mean	99% confidence limits on mean
polycarbonate	108	101–115
polyphenylene oxide	121	115–125
polyetherimide	93	90–96
polysulfone	121	114–128
PPO/polystyrene (75/25)[a]	206	193–218

[a] wt.%

TABLE VI
Critical aspect ratio for AS1 in thermoplastics

Matrix	Critical aspect ratio, l_c/d Mean	99% confidence limits on mean
polycarbonate	119	114–124
polyetherimide	84	80–88

TABLE VII
Critical aspect ratio for XAS in thermoplastic polymers

Matrix	Critical aspect ratio, l_c/d Mean	99% confidence limits on mean
polycarbonate	54	52–65
polyphenylene oxide	55	53–58
polyetherimide	55	52–57
polysulfone	55	(±19)[b]
PPO/polystyrene (75/25)[a]	61	58–64

[a] wt.%
[b] standard deviation.

The corresponding stress birefringence patterns for AS1, AS4 and XAS in polycarbonate are shown in Figure 8-10, respectively. The stress was increased from the upper left hand photograph to the lower right hand photograph in each figure. The photographs were not taken at the same fiber breaks but instead were taken to be representative of the birefringence at each stress level. Note that the initial birefringence node receded away from the fiber breaks with increasing

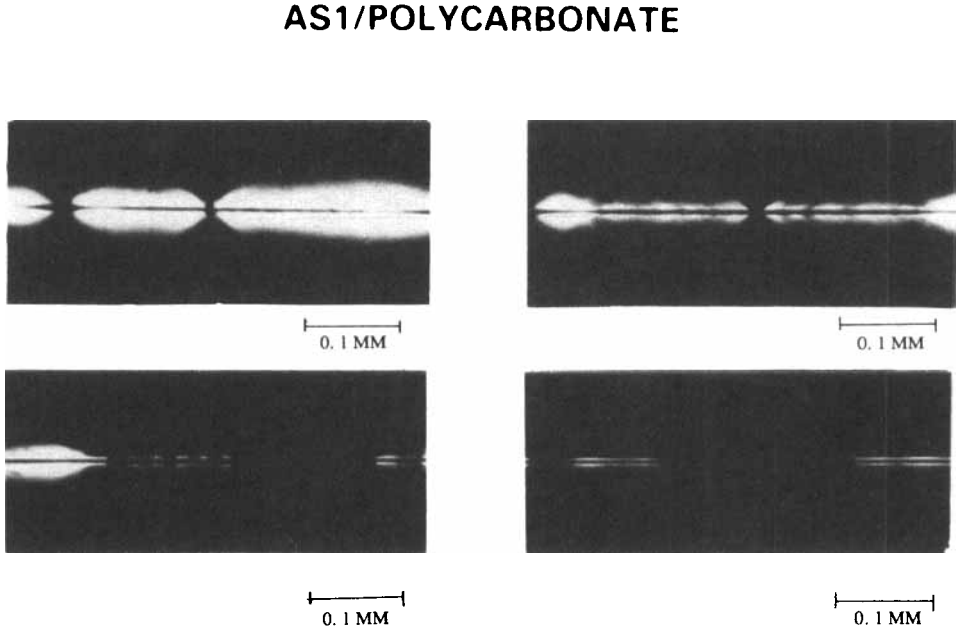

FIGURE 8 Stress birefringence at fiber breaks for AS1 in polycarbonate. Tensile stress increased from the upper left photograph to the lower right photograph.

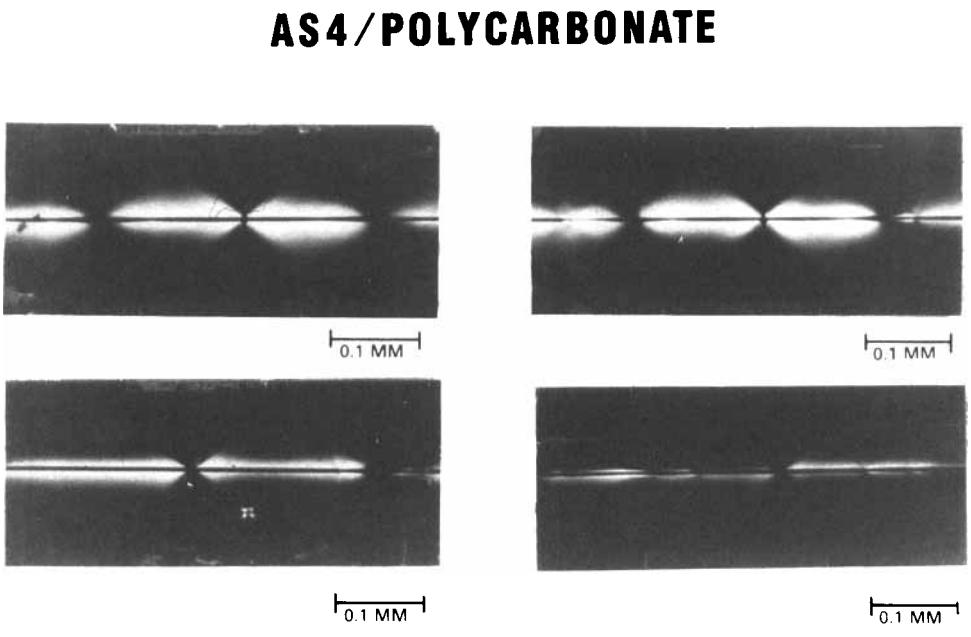

FIGURE 9 Stress birefringence at fiber breaks for AS4 in polycarbonate. Tensile stress increased from the upper left photograph to the lower right photograph.

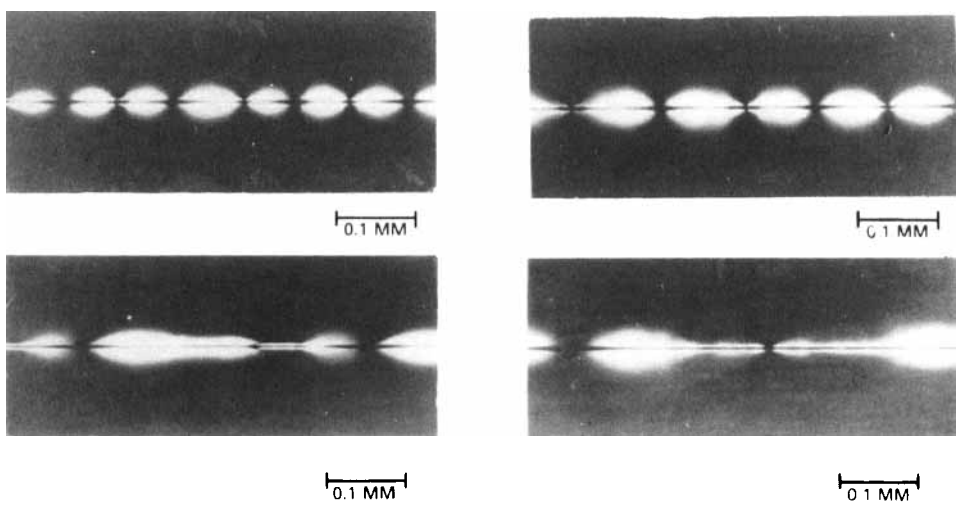

FIGURE 10 Stress birefringence at fiber breaks for XAS in polycarbonate. Tensile stress increased from the upper left photograph to the lower right photograph.

TABLE VIII
Effect of surface treatment on the critical length of AS4 in polycarbonate

Surface treatment level	Critical aspect r/atio
none	126
normal	100
4X normal	130

stress in the case of the AS1 and AS4 whereas a "lip" of birefringence develops in the case of the XAS. These stress birefringence observations are consistent with the critical aspect ratio results, *i.e.*, strong adhesion in the case of the XAS fiber and weak adhesion in the case of the AS1 and AS4 fibers. Very similar results were obtained for these fibers in the other thermoplastics.

The effect of surface treatment and sizings on the critical aspect ratios are listed in Tables VIII and IX respectively. The effects of surface cleaning by heat cleaning and solvent extraction on the critical length of AS4 in polycarbonate are listed in Table X.

The polycarbonate was fractionated using size exclusion chromatography. A small amount (~5%) of polymer having molecular weights less than 10^4 was removed. The effect of this fractionation on the critical aspect ratio of AS4 in polycarbonate is shown in Table XI.

The surfaces of the fibers were characterized from contact angle measurements,

TABLE IX
Effect of sizings on the critical length and critical aspect ratio of AS4 in polycarbonate

		Critical aspect ratio, l_c/d	
Sizing agent	Wt% on fiber	Mean	99% COLM[a]
none	—	108	101–195
W-size[b]	10	94	81–98
epoxy/anhydride[c]	0.45	114	110–118
aminopropylsilane[d]	0.12	99	94–103
phenoxy[e]	0.08	79	77–81
polycarbonate	0.10	115	110–119

[a] confidence limits on the mean.
[b] Hercules proprietary epoxy-based size.
[c] DGEBA/hexahydrophthalic anhydride.
[d] A-1100, Union Carbide Corp.
[e] PKHC, Union Carbide Corp.

TABLE X
Effect of solvent extraction and heat cleaning on the critical aspect ratio of AS4 in polycarbonate

	Critical aspect ratio, l_c/d	
Treatment	Mean	99% COLM[a]
none	108	101–115
THF[b]	130	122–135
heated at 750°C	100	—

[a] confidence limits on the mean.
[b] tetrahydrofuran.

X-ray photoelectron spectroscopy (XPS) and scanning electron microscopy. The wetting measurements proved to be so erratic as to be essentially useless. For example, the contact angle for α-bromonaphthalene ranged from 12° to 36° for AS4 and from 22° to 42° for the XAS fiber.

The XPS analysis results for the three fibers are presented in Table XII. There is no correlation between the surface elemental compositions and the critical lengths or critical aspect ratios. However, there does appear to be a correlation with the oxygen/nitrogen ratio as shown in Figure 11.

The fibers were examined using SEM and photomicrographs are presented in Figure 12. Striations were observed on both the AS1 and XAS which is not surprising since the polyacrylonitrile (PAN) precursor for these fibers is obtained from the same source. However, these striations have no relevance to the adhesion properties of the two fibers, in that the AS1 exhibited the lowest adhesion but the XAS exhibited the strongest adhesion as measured using the single embedded filament test.

A series of exploratory experiments were conducted to determine if the fibers differed in their adsorptivity of polycarbonate from an organic solvent. Weighed amounts of fiber were placed in flasks and equilibrated with polycarbonate in dichloroethane in flasks at a concentration of 0.2 mg/ml. Changes in polymer concentration *vs* time were measured by UV absorption at 265 nm. Despite experimental uncertainties due mostly to uncontrolled evaporation of the solvent,

TABLE XI
Effect of the fractionation of polycarbonate on the critical aspect ratio of AS4

	Critical aspect ratio	
Polycarbonate	Mean	99% COLM
as received	108	101–115
fractionated	133	110–124

TABLE XII
XPS Analysis of carbon fibers

	Elemental composition, %		
Fiber	Carbon	Oxygen	Nitrogen
AS1	81.0	11.2	5.6
AS4	88.6	7.6	3.8
XAS	80.5	10.5	7.9

the data at least suggested a greater adsorptivity by the XAS fiber than by the other two fibers.

To confirm this observation, retention time liquid chromatography experiments were conducted by injecting polycarbonate dissolved in dichloroethane (DCE) into a stream of DCE flowing through a column packed with carbon fiber (Figure 7). The results are listed in Table XIII and box plots of the data are presented in Figure 13. Clearly, there is a significant difference in the retention times. Moreover, the retention times correlate with the critical lengths in polycarbonate as shown in Figure 14. The greater the adsorptivity the lower the critical length and thus the stronger the adhesion.

DISCUSSION

In any effort to explain low adhesion between commercial materials, the first suspect is the presence of a weak boundary layer, resulting from surface contamination or the diffusion of contaminants or low MW components to the interface if one of the materials is initially a liquid. Cleaning of the fibers by heat treatment and solvent extraction had no effect on the adhesion of AS4 to

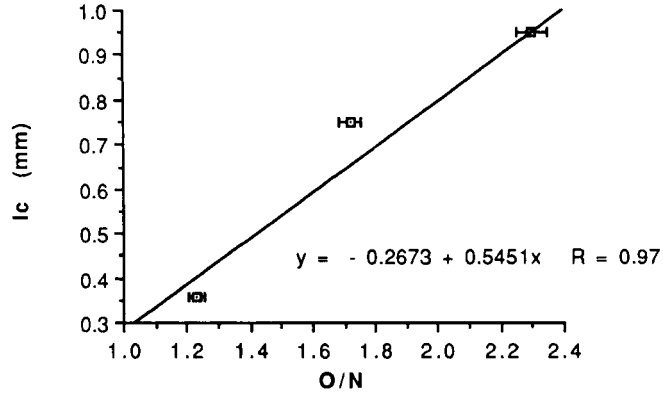

FIGURE 11 Correlation between the critical length of AS4 in polycarbonate and the XPS oxygen/nitrogen ratio.

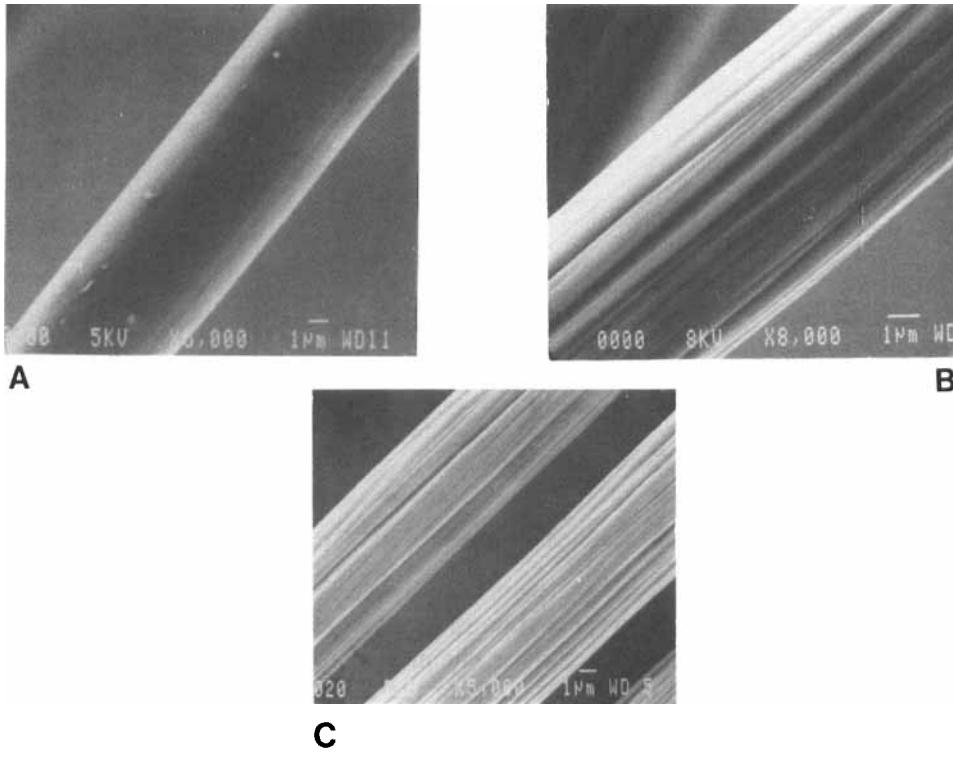

FIGURE 12 Scanning Electron photomicrographs of AS4(A), XAS(B) and AS1(C).

polycarbonate (Table X) which would appear to rule out fiber surface contamination. Similarly, fractionation of the polycarbonate (PC) to remove low MW species did not improve adhesion (Table XI) but, in fact, resulted in a larger critical aspect ratio than for the untreated PC.

Having eliminated the presence of a weak boundary layer, the next suspect is surface roughness. The SEM photographs in Figure 12 indicate distinctly different surface topography for the AS1 and XAS compared to AS4 but these differences are totally inconsistent with the differences in adhesion.

The surface treatment of carbon fibers ostensibly imparts a chemical "activa-

TABLE XIII
Retention time for polycarbonate in dichloroethane

Fiber	Retention time (min)
AS1	13.27 ± 0.07
AS4	13.67 ± 0.09
XAS	14.61 ± 0.12

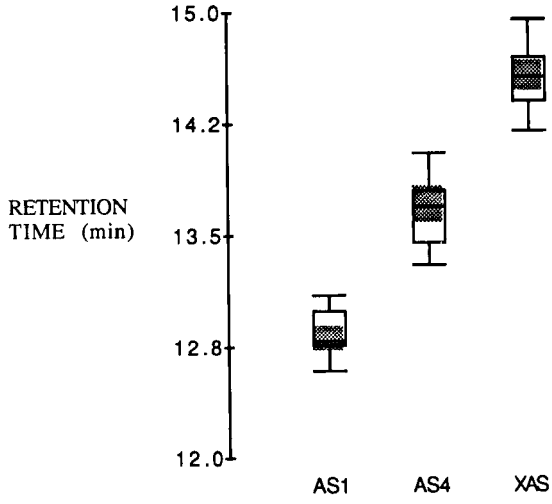

FIGURE 13 Statistical comparison of HPLC retention times.

tion" to the surface. Actually, it is is more of a surface cleaning operation which also probably "stabilizes" the surface chemical constitution to a reproducible condition. In Table VIII, wide variations in the surface treatement level did not improve the AS4/PC adhesion.

The sizings listed in Table IX were ineffective with the possible exception of the phenoxy coating. In fact, in various trials at different levels of phenoxy coatings, some specimens exhibited regions of strong adhesion, *i.e.*, low critical lengths and birefringence patterns characteristic of strong adhesion. However, the effect was not uniform and difficult to reproduce. Possibly, the sizing was not uniformly applied. In any future work phenoxy sizings should be reexamined.

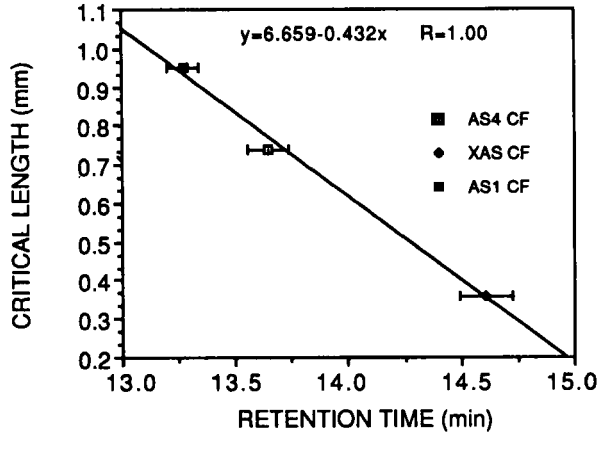

FIGURE 14 Correlation between critical lengths and polycarbonate retention times.

The surface characterization experiments, XPS and retention time chromatography suggest a subtle difference in the surface chemistry of the three fiber types. This tentative conclusion is based on the correlation between the critical length and O/N ratio determined using XPS (Figure 11) and the retention time (Figure 14). The correlation with the O/N ratio may be more fortuitous than real since some results from work in progress with other fibers do not fit this correlation.

The strongest evidence for a difference in the surface chemistries of the three fibers is the retention time chromatography results. This technique is very sensitive to surface chemical differences.

The origin of these differences in surface chemistry is probably related to the surface treatment methods used by the two manufacturers. Both Hercules Aerospace and Hysol Grafil (now Courtaulds Grafil) use an electrolytic oxidation treatment. However, it is extremely unlikely that they are identical. It is entirely possible, as suggested by one reviewer of this paper, that an interfacial crystallinity ($<0.5\ \mu$m thick) develops on some fibers and not others or that there are differences in submicron surface porosity. These are possible explanations that deserve further examination.

The relevance of these studies to the actual mechanical performance of composites is, of course, a critical issue. Recently, Hinkley *et al.*[15] compared the Mode I interlaminar fracture energy of laminates of AS4 and XAS in polyphenylene oxide (PPO). The value obtained for the AS4 was 240 J/m^2 compared with 440 J/m^2 for the XAS composite. Evidently, the strong adhesion of the XAS to the PPO had a marked effect on the delamination energy compared with the weakly-bonded AS4/PPO composite.

Strictly speaking, the results reported here are relevant to the "wet-winding" processing where the carbon fibers are impregnated with the matrix polymer from solution. We are convinced that the drying procedures used here allowed complete evaporation of the solvent from the test specimens. It was impractical to make these specimens using molten polymers due to the high thermal compressive stresses that develop on cool-down. None the less, there is evidence in the literature of low adhesion between carbon fibers in composites processed by hot-melt techniques. Scanning electron microscopy of a fractured specimen of polyphenylene sulfide (PPS)-AS4 composite strongly indicated very low adhesion.[1] Although SEM is not always a reliable means of detecting interfacial failure, the appearance of the PPS-AS4 material was dramatically different from SEM images of composites where the matrix is known to adhere to the fiber.

CONCLUSION

Studies using the embedded single fiber test for carbon fiber/polymer adhesion have quantitatively confirmed the low adhesion of these fibers to thermoplastic polymers. However, of the three fiber types tested, AS1, AS4, and XAS, the XAS exhibited strong adhesion to all of the thermoplastics. Possible explanations for this difference between the AS fibers and the XAS such as weak boundary

layers and differences in surface roughness were eliminated. Also, different fiber surface treatment levels and various sizings were ineffective in promoting adhesion of the AS4.

Surface analysis using XPS and liquid retention time chromatography suggest minor differences in the surface chemical constitution of the fibers and these differences correlate with the adhesion of the AS4 fiber to polycarbonate. Work is in progress to characterize better the surface composition of the fibers.

Finally, a correlation between fiber matrix adhesion as determined by the embedded filament test and interlaminar fracture has been recently reported.[15]

Acknowledgements

The authors wish to thank the National Aeronautical and Space Administration for financial support of this work. Special thanks are due to Drs. N. J. Johnston and J. A. Hinkley of the NASA Langley Research Center (Hampton, VA, U.S.A.) for their suggestions, advice and especially their patience through the course of this investigation. We also wish to thank Neil Hansen and David Boll (Hercules Aerospace) for helpful discussions and suggestions.

References

1. W. D. Bascom, D. J. Boll, B. Fuller, and P. J. Phillips, *J. Mat. Sci.* **20,** 3184 (1985).
2. W. L. Bradley, and R. N. Cohen, *Delamination and Debonding of Materials,* STP 876, W. S. Johnson, Ed. (American Society for Testing and Materials, Philadelphia, PA, U.S.A. 1985), p. 389.
3. D. L. Hunston, R. J. Moulton, N. J. Johnston and W. D. Bascom, *Toughened Composites,* STP 937, N. J. Johnston, Ed. (American Society for Testing and Materials, Philadelphia, PA, U.S.A. 1987), p. 74.
4. W. D. Bascom and S. Y. Gweon, in *Fractography and Failure Mechanisms of Polymers and Composites,* A. C. Roulin-Moloney, Ed. (Elsevier, NY, 1989), p. 351.
5. W. D. Bascom, unpublished results.
6. A. Kelly and W. R. Tyson, *Mech. Phys. Solids* **13,** 329 (1965).
7. W. A. Fraser, F. H. Ancker, A. T. DiBenedetto, and B. Elbirli, *Polym. Comp.* **4,** 238 (1983).
8. W. A. Fraser, F. H. Ancker, and A. T. DiBenedetto, *Proc. Conf. on Reinforced Plastics,* Soc. Plastics Ind., 1975, Section 22A, p. 1.
9. L. T. Drzal, M. J. Rich, and P. F. Lloyd, *J. Adhesion* **16,** 1 (1983).
10. L. T. Drzal, M. J. Rich, M. F. Koenig, and P. F. Lloyd, *J. Adhesion* **16,** 133 (1982).
11. W. D. Bascom, and R. M. Jensen, *J. Adhesion* **19,** 219 (1986).
12. A. Kelly, *Strong Solids* (Clarendon Press, Oxford, 1973), p. 172.
13. W. D. Bascom, "Interfacial Adhesion of Carbon Fibers," Final Report of NASA Contract NAS1-17918, April 15, 1987.
14. K. B. Sentell and J. G. Dorsey, *J. of Chromatography* **4610,** 193 (1989).
15. J. A. Hinkley, W. D. Bascom, and R. E. Allred, "Interlaminar Fracture in Carbon/Fiber Thermoplastic Composites", Proc. of the 1989 Sym. on Tailored Interfaces in Composite Materials, Materials Research Soc., Boston, MA, 1990.